

Coherence resonance for time-averaged measures

Go Uchida

Department of Mechanical Systems Engineering, Tokyo Metropolitan University, Tokyo 1920397, Japan

(Dated: October 5, 2023)

Noise can induce time order in the dynamics of nonlinear dynamical systems. For example, coherence resonance occurs in various neuron models driven by a noise. In studies of coherence resonance, ensemble-averaged measures of the coherence are often used. In the present study, we examine coherence resonance for time-averaged measures. For the examination, we use a Hodgkin-Huxley neuron model driven by a constant current and a noise. We firstly show that for large times, the neuron is in a stationary state irrespective of initial conditions of the neuron. We then show numerical evidence that in the stationary state, a given noise sample path uniquely determines the dynamics of the neuron. We then present numerical evidence suggesting that time-averaged coherence measures of the dynamics is independent of noise sample paths and is equal to ensemble-averaged coherence measures. On the basis of this property, we show that coherence resonance is not only a phenomenon related to ensemble-averaged measures but also a phenomenon that holds for time-averaged measures.

I. INTRODUCTION

Noise has unexpected effects on responses of nonlinear systems. Coherence resonance is an example. When an autonomous nonlinear system is driven by an external noise, regularity of its periodic response is maximal at a certain noise level. Coherence resonance was firstly found in a model of a simple autonomous system [1]. Subsequently, it was found in the Plant model (a model for a bursting neuron) [2], a FitzHugh-Nagumo model [3], a Hodgkin-Huxley model [4], laser models [5, 6], and a semiconductor superlattice model [7]. Coherence resonance was observed not only in models but also in experiments [8–12].

In studies of coherence resonance, measures of the regularity are often estimated by the ensemble average [3, 4, 13]. However, for comparison with experiments, it may be rather important that coherence resonance holds for time-averaged measures. Nevertheless, it is not necessarily clear whether coherence resonance also holds for time-averaged measures.

In the present study, we examine coherence resonance for time-averaged measures. In the examination, we use a Hodgkin-Huxley neuron model driven by a constant current and a noise.

This paper is organized as follows: In Sec. II, we describe a Hodgkin-Huxley neuron model we use. The model is described by a set of stochastic differential equations. In Sec. III, some concepts of the theory of random dynamical systems are briefly explained. The theory of random dynamical systems provides a framework for pathwise analysis of stochastic differential equations. We also briefly review the dynamical behaviors of the Hodgkin-Huxley neuron. In Sec. IV, we examine coherence resonance of the Hodgkin-Huxley neuron for time-averaged measures. In Sec. V, we discuss the results.

II. MODEL

We use a Hodgkin-Huxley neuron model driven by a constant current and a noise. The electrophysiological activity of the Hodgkin-Huxley neuron is given by

$$C \frac{dv}{dt} = -g_{Na} m^3 h (v - V_{Na}) - g_K n^4 (v - V_K) - g_L (v - V_L) + I + \sigma \xi(t), \quad (1a)$$

$$\frac{dm}{dt} = \alpha_m(v)(1 - m) - \beta_m(v)m, \quad (1b)$$

$$\frac{dh}{dt} = \alpha_h(v)(1 - h) - \beta_h(v)h, \quad (1c)$$

$$\frac{dn}{dt} = \alpha_n(v)(1 - n) - \beta_n(v)n, \quad (1d)$$

where v represents the membrane potential; C is the membrane capacitance; g_{Na} , g_K , and g_L are the maximum conductance for sodium ion, potassium ion, and leakage channels, respectively; V_{Na} , V_K , and V_L are the reversal potentials; m , n , and h are the gating variables. In Eqs. (1b) to (1d), $\alpha_m(v)$, $\alpha_h(v)$, $\alpha_n(v)$, $\beta_m(v)$, $\beta_h(v)$ and $\beta_n(v)$ are the voltage-dependent rate constants. The voltage-dependent rate constants have the form [14]:

$$\alpha_m(v) = \frac{0.1(v + 40)}{1 - \exp[-(v + 40)/10]}, \quad (2a)$$

$$\beta_m(v) = 4 \exp[-(v + 65)/18], \quad (2b)$$

$$\alpha_h(v) = 0.07 \exp[-(v + 65)/20], \quad (2c)$$

$$\beta_h(v) = \frac{1}{1 + \exp[-(v + 35)/10]}, \quad (2d)$$

$$\alpha_n(v) = \frac{0.01(v + 55)}{1 - \exp[-(v + 55)/10]}, \quad (2e)$$

$$\beta_n(v) = 0.125 \exp[-(v + 65)/80]. \quad (2f)$$

In Eq. (1a), I represents a constant external current and $\xi(t)$ represents a Gaussian white noise: $\langle \xi(t) \rangle = 0$ and $\langle \xi(t)\xi(t') \rangle = \delta(t - t')$. The symbol σ represents the amplitude of the noise.

III. PRELIMINARIES

A. Some concepts of the theory of random dynamical systems

In the present study, we use some concepts of the theory of random dynamical systems. The theory of random dynamical systems provides a framework for path-wise analysis of stochastic differential equations. Here, a brief explanation of the concepts is given. More detailed and rigorous descriptions of the concepts can be found in [15].

1. Pullback method, random attractor, and invariant measure

Here, we focus on the systems described by stochastic differential equations as random dynamical systems, although random dynamical systems include systems not described by stochastic differential equations.

We assume that the dynamics of a system is described by a stochastic differential equation:

$$\frac{dx}{dt} = f(x) + \sigma\xi(t). \quad (3)$$

We denote a formal solution of Eq. (3) for a given noise sample path ω as $x(t, \omega)$ and the initial condition as x_0 . In the field of random dynamical systems, the solution $x(t, \omega)$ is expressed as $\varphi(t, \omega)x_0$ using a map $\varphi(t, \omega)$.

A random attractor \mathcal{A} is defined as $\mathcal{A} = \{A(\omega)\}_{\omega \in \Omega}$ where Ω represents the set of all ω , and $A(\omega)$ is defined as a φ -invariant set that attracts, in a pullback sense, all points in a region of the phase space. Here, φ -invariant means that the following equation holds:

$$\varphi(t, \omega)A(\omega) = A(\theta_t\omega), \quad (4)$$

where θ_t represents the shift operator and maps $\xi(s; \omega)$ to $\xi(s+t; \omega)$. It is known that for a Gaussian white noise, θ_t is a bijection from Ω to Ω .

The pullback means $\lim_{t \rightarrow \infty} \varphi(t, \theta_{-t}\omega)x_0$. This corresponds to characterizing the asymptotic behavior of the system by the time evolution from $t = -\infty$ to $t = 0$ instead of the time evolution from $t = 0$ to $t = \infty$. The reason for using the pullback will become clear in the next section (Sec. III A 2).

Random dynamical systems do not necessarily have random attractors. A random dynamical system possesses a random attractor if all trajectories starting at $t' = -\infty$ are within a bounded region $B(\omega)$ at the time $t = 0$ [15–17].

From the point of view of probability theory, if a random dynamical system has a random attractor, then the system almost surely has a φ -invariant conditional probability given a noise sample path ω [15, 16]:

$$\mu_\omega(A(\omega)) = 1, \quad (5)$$

where μ_ω represents the φ -invariant conditional probability given a noise sample path ω . The probability μ_ω is called an invariant measure.

For a random dynamical system, the invariant measure and the stationary solution of the Fokker-Planck equation for the system have one-to-one correspondence [15, 16]:

$$\mathbb{E}_\omega[\mu_\omega(dx)] = \rho(x)dx, \quad (6)$$

$$\lim_{t \rightarrow \infty} \varphi(t, \theta_{-t}\omega)\rho(x)dx = \mu_\omega(dx), \quad (7)$$

where \mathbb{E}_ω represents the expectation and $\rho(x)$ is a solution of the equation:

$$\left[-\frac{\partial}{\partial x}f(x) + \frac{\sigma^2}{2} \frac{\partial^2}{\partial x^2} \right] \rho(x) = 0. \quad (8)$$

The point in this section is that for large times, the system is in a stationary state irrespective of initial conditions if the system has a random attractor.

2. Example

Here, a simple example is provided to facilitate understanding of the concepts explained in the previous section. The theory of random dynamical systems is applicable not only to nonlinear systems with a noise but also to linear systems with a noise. For simplicity, we use a linear system with a noise as an example. The example we use is as follows:

$$\frac{dx}{dt} = -\gamma x + \sigma\xi(t), \quad (9)$$

where γ is a positive constant.

For a given noise sample path ω , a formal solution of Eq. (9) is given by

$$\varphi(t, \omega)x_0 = e^{-\gamma t}x_0 + \sigma \int_0^t e^{-\gamma(t-s)}\xi(s; \omega)ds. \quad (10)$$

From Eq. (10), we can see that $\lim_{t \rightarrow \infty} \varphi(t, \omega)x_0$ is indeterminate. This makes it difficult to characterize asymptotic behaviors of the system. However, this difficulty is overcome by using the pullback. For the system given by Eq. (9), we have the pullback:

$$\lim_{t \rightarrow \infty} \varphi(t, \theta_{-t}\omega)x_0 = \sigma \int_{-\infty}^0 e^{\gamma s}\xi(s; \omega)ds. \quad (11)$$

This pullback is bounded because $\varphi(t, \omega)x_0$ is an Ornstein-Uhlenbeck process. We denote the limit in Eq. (11) as $x^*(\omega)$.

The system given by Eq. (9) has a random attractor because the pullback is bounded. In addition, all solutions converge to $x^*(\omega)$ irrespective of initial conditions and $x^*(\omega)$ is φ -invariant (see Appendix A):

$$\varphi(t, \omega)x^*(\omega) = x^*(\theta_t\omega). \quad (12)$$

The random attractor $A(\omega)$ is given by

$$A(\omega) = \{x^*(\omega)\}. \quad (13)$$

If a random attractor is the family of singletons, the attractor is called a random point attractor.

From Eqs. (5) and (13), an invariant measure for the system given by Eq. (9) is given by

$$\mu_\omega = \delta_{x^*(\omega)}. \quad (14)$$

The measure $\delta_{x^*(\omega)}$ is called a random Dirac measure and is given by $\delta_{x^*(\omega)} = \delta(x - x^*(\omega)) dx$.

The stationary solution of the Fokker-Planck equation for the system described by Eq. (9) is given by

$$\rho(x) = \frac{1}{\sqrt{\pi}\sigma} \exp\left(-\frac{x^2}{\sigma^2}\right). \quad (15)$$

Thus, from Eq. (6), we have

$$\mathbb{E}_\omega [\delta_{x^*(\omega)}] = \frac{1}{\sqrt{\pi}\sigma} \exp\left(-\frac{x^2}{\sigma^2}\right) dx. \quad (16)$$

The point in this section is that if a random attractor of a system is a random point attractor, in the stationary state, a given noise sample path uniquely determines the dynamics of the system.

B. Dynamical behaviors of the Hodgkin-Huxley neuron

Here, we briefly review the dynamics of the Hodgkin-Huxley neuron given by Eqs. (1a) to (2f) to clarify the regions of I and σ where coherence resonance occurs.

When $\sigma = 0$, in the Hodgkin-Huxley neuron given by Eqs. (1a) to (2f), a saddle-node bifurcation of periodic orbits occurs at $I = 6.23 \mu\text{A}/\text{cm}^2$ and a Hopf bifurcation occurs at $I = 9.78 \mu\text{A}/\text{cm}^2$. For $I < 6.23 \mu\text{A}/\text{cm}^2$, a stable fixed point is the only attractor. For $6.23 \mu\text{A}/\text{cm}^2 < I < 9.78 \mu\text{A}/\text{cm}^2$, a stable fixed point, a stable limit cycle, and an unstable limit cycle coexist and the unstable limit cycle is the separatrix between the stable fixed point and the stable limit cycle. For $9.78 \mu\text{A}/\text{cm}^2 < I$, a stable limit cycle is the only attractor.

When $I < 6.23 \mu\text{A}/\text{cm}^2$, moderate to high amplitude noise induces stochastic firing in the Hodgkin-Huxley neuron given by Eqs. (1a) to (2f). This stochastic firing is based on excitable dynamics: noise makes the neuron an excursion into the region of the limit cycle. In this region of the input parameters, coherence resonance is observed [13].

IV. RESULTS

In this section, we firstly show analytically that the Hodgkin-Huxley neuron has a random attractor and then

TABLE I. Values of the model parameters

Parameters	Values
C	$1 \mu\text{F}/\text{cm}^2$
g_{Na}	$120 \text{ mS}/\text{cm}^2$
g_K	$36 \text{ mS}/\text{cm}^2$
g_L	$0.3 \text{ mS}/\text{cm}^2$
V_{Na}	50 mV
V_K	-77 mV
V_L	-54.4 mV

show numerically that the attractor is a random point attractor. We then characterize the dynamics in the stationary state and examine coherence resonance for time-averaged measures.

A. Existence of a random attractor

The Hodgkin-Huxley neuron given by Eqs. (1a) to (2f) has a random attractor and thus for large times, the neuron is in a stationary state irrespective of initial conditions. The gating variables m , h , and n are always bounded between zero and one irrespective of the noise sample path ω . In addition, the pullback of v is also bounded (see Appendix B). Here, it is worth noting that the existence of a random attractor does not depend on the values of I and σ .

B. Structure of the random attractor

We next show numerical evidence that the random attractor is a random point attractor in a parameter range where coherence resonance occurs. The initial conditions for the numerical calculations are given in a grid form over a wide region of the phase space: the initial conditions are all possible combinations of $v_i = V_K + i(V_{Na} - V_K)/5$ ($i = 0, 1, \dots, 5$), $m_j = 0 + j/4$ ($j = 0, 1, \dots, 4$), $h_k = 0 + k/4$ ($k = 0, 1, \dots, 4$), and $n_l = 0 + l/4$ ($l = 0, 1, \dots, 4$); the number of the initial conditions are 750. The values of the model parameters we use in calculations are shown in Table I.

In the present study, we fix the value of I to $6.2 \mu\text{A}/\text{cm}^2$ and change the value of σ . We firstly set $\sigma = 10 \mu\text{A} \cdot \text{ms}^{1/2}/\text{cm}^2$. Figure 1 shows the pullbacks projected onto v - n plane. The projected points converge to a single point irrespective of the initial conditions. The result is the same for the pullbacks projected onto the other planes. These results mean that the trajectories in the phase space converge to a single trajectory irrespective of the initial conditions. For other sample paths of $\xi(t)$, we have the same result. These results suggest that the random attractor is a random point attractor and thus for a given noise sample path, the dynamics of the neuron is uniquely determined in the stationary state.

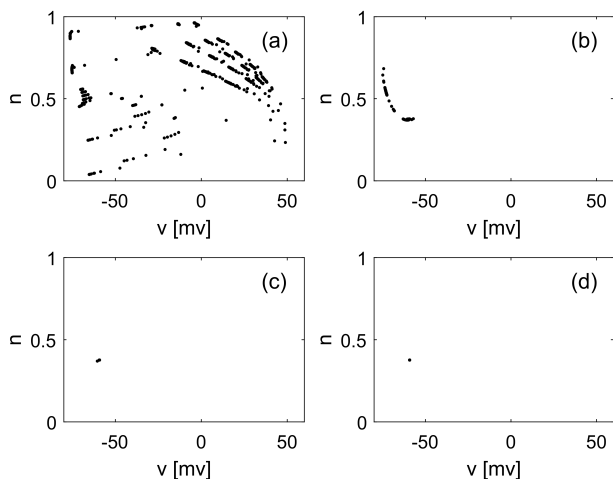


FIG. 1. Pullbacks of the Hodgkin-Huxley neuron for a sample path of $\xi(t)$. $I = 6.2 \mu\text{A}/\text{cm}^2$ and $\sigma = 10 \mu\text{A} \cdot \text{ms}^{1/2}/\text{cm}^2$. (a) $t = 1$ ms. (b) $t = 200$ ms. (c) $t = 500$ ms. (d) $t = 2000$ ms.

For other values (6, 8, 20, 40, 60, 80, and $100 \mu\text{A} \cdot \text{ms}^{1/2}/\text{cm}^2$) of σ , we obtain the same result: the trajectories in the phase space converge to a single trajectory irrespective of the initial conditions. This result suggests that the random attractor is also a random point attractor for those values of σ and thus for a given noise sample path, the dynamics of the neuron is uniquely determined in the stationary state.

C. Dynamics in the stationary state

Unfortunately, the theory of random dynamical systems does not provide analytical methods to obtain further insight into the dynamics in the stationary state.

Figure 2 shows the time courses of v in the stationary state for $\sigma = 10 \mu\text{A} \cdot \text{ms}^{1/2}/\text{cm}^2$ and $\sigma = 40 \mu\text{A} \cdot \text{ms}^{1/2}/\text{cm}^2$. We can see that the membrane potentials show intermittent oscillations for both values of σ . Interestingly, however, the oscillations appear to be more regular at $\sigma = 40 \mu\text{A} \cdot \text{ms}^{1/2}/\text{cm}^2$ than at $\sigma = 10 \mu\text{A} \cdot \text{ms}^{1/2}/\text{cm}^2$.

We then quantify the irregularity of the intermittent oscillation. We cut the random point attractor by a section $v = -40$ mV, $0.1 \leq m \leq 0.4$, $0.2 \leq h \leq 0.8$, $0.1 \leq n \leq 0.6$ (Poincaré section). For a given noise sample path ω , we denote the n -th recurrence time of the neuron to the Poincaré section as $T_n(\omega)$. We define the time-averaged irregularity of an oscillation as

$$\bar{R}(\omega) = \frac{\sqrt{\overline{T^2(\omega)} - [\overline{T(\omega)}]^2}}{\overline{T(\omega)}}, \quad (17)$$

where $\bar{R}(\omega)$ represents the time-averaged irregularity of

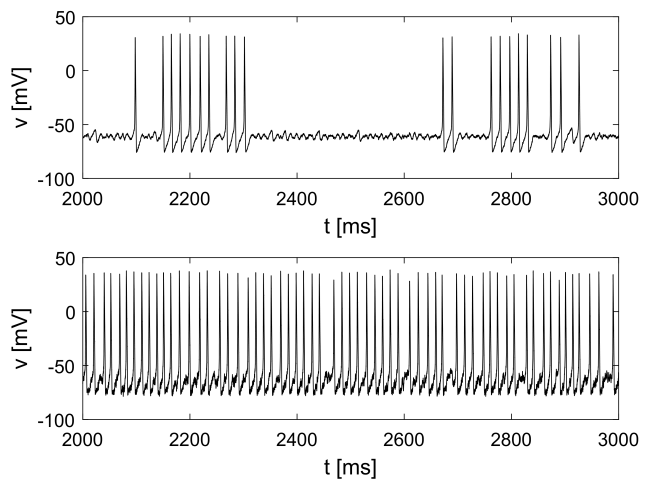


FIG. 2. Time courses of the membrane potentials. $I = 6.2 \mu\text{A}/\text{cm}^2$. Top panel: $\sigma = 10 \mu\text{A} \cdot \text{ms}^{1/2}/\text{cm}^2$, Bottom panel: $\sigma = 40 \mu\text{A} \cdot \text{ms}^{1/2}/\text{cm}^2$.

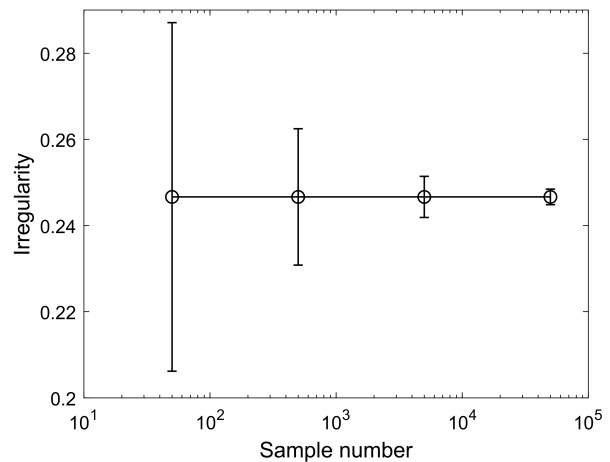


FIG. 3. The dependence of the difference between the time-averaged and the ensemble-averaged irregularity on the sample number of the recurrence times. $I = 6.2 \mu\text{A}/\text{cm}^2$ and $\sigma = 40 \mu\text{A} \cdot \text{ms}^{1/2}/\text{cm}^2$. The open circles represent the ensemble-averaged irregularity. The error bars represent standard deviation $S_R(N)$. The solid line is a guide for eyes.

an oscillation. In Eq. (17), $\bar{T}(\omega)$ and $\overline{T^2}(\omega)$ are given by

$$\bar{T}(\omega) = \lim_{N \rightarrow \infty} \frac{1}{N} \sum_{n=1}^N T_n(\omega), \quad (18)$$

$$\overline{T^2}(\omega) = \lim_{N \rightarrow \infty} \frac{1}{N} \sum_{n=1}^N T_n^2(\omega). \quad (19)$$

If an attractor is a deterministic limit cycle, the recurrence time is a constant regardless of n and thus $\bar{R}(\omega) = 0$. On the other hand, when the recurrence time follows an exponential distribution, $\bar{R}(\omega) = 1$.

Here, we also define the ensemble-averaged irregularity

of an oscillation $\langle R(\omega) \rangle$:

$$\langle R(\omega) \rangle = \frac{\sqrt{\langle T_1^2(\omega) \rangle - \langle T_1(\omega) \rangle^2}}{\langle T_1(\omega) \rangle}. \quad (20)$$

Figure 3 shows the sample number N dependence of the standard deviation $S_R(N)$. Here, the standard deviation $S_R(N)$ is given by

$$S_R(N) = \sqrt{\left\langle \left(\widehat{R}(N, \omega) - \langle R(\omega) \rangle \right)^2 \right\rangle}, \quad (21)$$

where $\widehat{R}(N, \omega)$ is an estimate of $\overline{R}(\omega)$ and is given by

$$\widehat{R}(N, \omega) = \frac{\sqrt{\widehat{T}^2(N, \omega) - [\widehat{T}(N, \omega)]^2}}{\widehat{T}(N, \omega)}. \quad (22)$$

In this equation, $\widehat{T}(N, \omega)$ and $\widehat{T}^2(N, \omega)$ are given by

$$\widehat{T}(N, \omega) = \frac{1}{N} \sum_{n=1}^N T_n(\omega), \quad (23)$$

$$\widehat{T}^2(N, \omega) = \frac{1}{N} \sum_{n=1}^N T_n^2(\omega). \quad (24)$$

From Fig. 3, we can see that the standard deviation monotonically decreases as the sample number increases. This result suggests that $\overline{R}(\omega)$ is independent of ω and is equal to $\langle R(\omega) \rangle$.

In the following, we simply denote the irregularity as R , but the estimation is based on the time average. As we have just shown, for $\sigma = 40 \mu\text{A} \cdot \text{ms}^{1/2}/\text{cm}^2$, $R = 0.2465$. On the other hand, for $\sigma = 10 \mu\text{A} \cdot \text{ms}^{1/2}/\text{cm}^2$, $R = 1.1385$. The value of R is smaller for $\sigma = 40 \mu\text{A} \cdot \text{ms}^{1/2}/\text{cm}^2$ than for $\sigma = 10 \mu\text{A} \cdot \text{ms}^{1/2}/\text{cm}^2$. This result is consistent with the result obtained by the comparison in Figure 2.

Figure 4 shows the dependence of the irregularity R on σ for different sample paths of $\xi(t)$. The curves overlap well and are downward convex. The irregularity R is minimal at $\sigma = 60 \mu\text{A} \cdot \text{ms}^{1/2}/\text{cm}^2$. This is exactly the coherence resonance.

In studies of coherence resonance, the characteristic correlation time of the autocorrelation function is also used to evaluate the regularity [3, 13]. For a stationary stochastic process $y(t)$, the characteristic correlation time τ_c is defined as

$$\tau_c = \int_0^\infty C^2(t) dt. \quad (25)$$

In this equation, $C(t)$ is the autocorrelation function of $y(t)$ and is given by

$$C(\tau) = \frac{\langle (y(t) - \langle y \rangle)(y(t + \tau) - \langle y \rangle) \rangle}{\langle (y(t) - \langle y \rangle)^2 \rangle}, \quad (26)$$

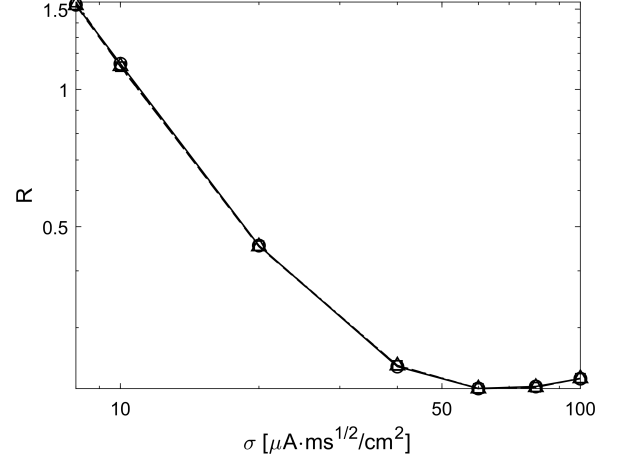


FIG. 4. The dependence of R on σ for $I = 6.2 \mu\text{A}/\text{cm}^2$. Different symbols (circles, triangles, and squares) represent the results for different sample paths of $\xi(t)$. The lines (solid, broken, and dash-dot) are a guide for eyes. The irregularity R was estimated from a minimum of 15 057 and a maximum of 71 687 samples of the recurrence times.

where τ represents the time difference. The characteristic correlation time τ_c takes a larger value as $y(t)$ shows a more regular oscillation.

In the stationary state, for the membrane potential, the autocorrelation function corresponding to Eq. (26), $C_v(\tau)$, is given by

$$C_v(\tau) = \frac{\langle (v^*(\omega) - \langle v^*(\omega) \rangle)(v^*(\tau, \omega) - \langle v^*(\omega) \rangle) \rangle}{\langle (v^*(\omega) - \langle v^*(\omega) \rangle)^2 \rangle}. \quad (27)$$

In this equation, $v^*(\omega)$ and $v^*(\tau, \omega)$ are given by

$$v^*(\omega) = \lim_{t \rightarrow \infty} \varphi_{hh}(t, \theta_{-t}\omega)v_0, \quad (28)$$

$$v^*(\tau, \omega) = \varphi_{hh}(\tau, \omega)v^*(\omega), \quad (29)$$

where v_0 is the initial condition of v and φ_{hh} is a map that provides the solution of Eqs. (1a) to (2f). On the other hand, for a given noise sample path ω , the time-averaged autocorrelation function of $v(t, \omega)$, $\overline{C}_v(\tau, \omega)$, can be defined as

$$\overline{C}_v(\tau, \omega) = \lim_{T' \rightarrow \infty} \frac{1}{T'} \int_0^{T'} v^*(t, \omega)v^*(t + \tau, \omega) dt. \quad (30)$$

Figure 5 shows the dependence of the standard deviation $S_C(T')$ on T' . Here, the standard deviation $S_C(T')$ is given by

$$S_C(T') = \lim_{\tau_u \rightarrow \infty} \frac{1}{\tau_u} \int_0^{\tau_u} \left\langle \left(\widehat{C}_v(\tau, T', \omega) - C_v(\tau) \right)^2 \right\rangle d\tau, \quad (31)$$

where $\widehat{C}_v(\tau, T', \omega)$ is an estimate of $\overline{C}_v(\tau, \omega)$ and is given by

$$\widehat{C}_v(\tau, T', \omega) = \frac{1}{T'} \int_0^{T'} v^*(t, \omega)v^*(t + \tau, \omega) dt. \quad (32)$$

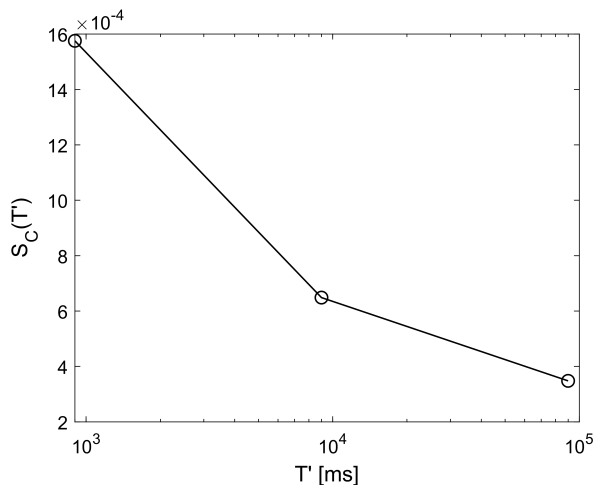


FIG. 5. The dependence of $S_C(T')$ on T' . $I = 6.2 \mu\text{A}/\text{cm}^2$ and $\sigma = 10 \mu\text{A} \cdot \text{ms}^{1/2}/\text{cm}^2$. The solid line is a guide for eyes.

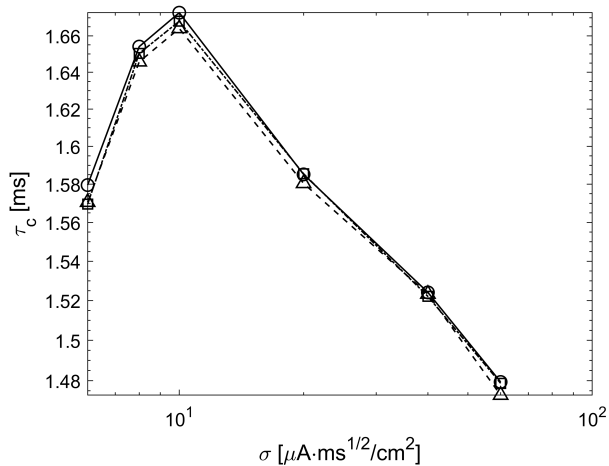


FIG. 6. The dependence of τ_c on σ for $I = 6.2 \mu\text{A}/\text{cm}^2$. Different symbols (circles, triangles, and squares) represent the results for different sample paths of $\xi(t)$. The lines (solid, broken, and dash-dot) are a guide for eyes. The autocorrelation functions of $v(t, \omega)$ were estimated from simulations lasting a minimum of 1 000 000 ms and a maximum of 8 000 000 ms, from which the starting 2 000 ms were discarded.

We can see that the standard deviation monotonically decreases as T' increases. This result suggests that $C_v(\tau, \omega)$ is independent of ω and is equal to $C_v(\tau)$.

In the following, the characteristic correlation time for $v(t)$ is evaluated based on the time-averaged autocorrelation function of $v(t, \omega)$. Figure 6 shows the dependence of the characteristic correlation time τ_c on σ for different sample paths of $\xi(t)$. The curves overlap well and are upward convex. The characteristic correlation time τ_c is maximal at $\sigma = 10 \mu\text{A} \cdot \text{ms}^{1/2}/\text{cm}^2$. This is also the coherence resonance.

V. DISCUSSION

In the present study, we examined coherence resonance for time-averaged measures of the regularity. In the examination, we used a Hodgkin-Huxley neuron model driven by a constant current and a noise. We showed that for large times, the neuron is in a stationary state irrespective of initial conditions. We then showed numerical evidence that in the stationary state, a given noise sample path uniquely determines the dynamics of the neuron. We then showed numerical evidence suggesting that the time-averaged measures of the regularity of the dynamics is independent of noise sample paths and equal to the ensemble-averaged measures. In addition, we demonstrated coherence resonance for time-averaged measures.

The irregularity of an oscillation R is equivalent to the coefficient of variation (CV) of interspike intervals, which is often used in the study of coherence resonance [3, 13]. We denote the value of v on the Poincaré section as v_p . We define the generation time of action potential as the time when the membrane potential v exceeds v_{th} . When $v_{th} = v_p$, the intervals between the generation times (interspike intervals) are equal to the recurrence times to the Poincaré section. In addition, the CV of interspike intervals is defined as the standard deviation of interspike intervals divided by the mean of interspike intervals. Thus, R is equal to CV of interspike intervals. This relation clarifies a nonlinear dynamical meaning of CV of interspike intervals: the variation of the recurrence times to a Poincaré section.

A Poincaré section is usually used to construct a Poincaré map. The Poincaré map is useful for clarifying qualitative properties of $(n + 1)$ -dimensional continuous dynamical systems governed by differential equations using n -dimensional discrete dynamical system theory. On the other hand, in the present study, the Poincaré section is used to reduce the four-dimensional continuous stochastic process to a one-dimensional point process. This reduction enables us to characterize the dynamics of high-dimensional continuous dynamical systems from the properties of low-dimensional simple stochastic processes.

In studies of coherence resonance, not only CV of interspike intervals and the characteristic correlation time but also the power spectrum is used to evaluate the regularity of the dynamics [4]. In the present study, numerical evidence suggested that the time-averaged autocorrelation function is independent of noise sample paths and equal to the ensemble-averaged autocorrelation function. The same is true for the power spectrum because the autocorrelation function and the power spectrum have a one-to-one relation by the Wiener-Khinchin theorem.

Appendix A: Proof of Eq. (12)

Here, we prove Eq. (12). Substituting $x_0 = \sigma \int_{-\infty}^0 e^{\gamma s} \xi(s; \omega) ds$ into the right hand side of Eq. (10) leads to

$$\begin{aligned} \varphi(t, \omega) x^*(\omega) &= \sigma e^{-\gamma t} \int_{-\infty}^0 e^{\gamma s} \xi(s; \omega) ds \\ &\quad + \sigma \int_0^t e^{-\gamma(t-s)} \xi(s; \omega) ds \\ &= \sigma \int_{-\infty}^t e^{-\gamma(t-s)} \xi(s; \omega) ds \\ &= \sigma \int_{-\infty}^0 e^{\gamma s} \xi(s+t; \omega) ds \\ &= x^*(\theta_t \omega). \end{aligned}$$

Appendix B: Boundedness of the pullback of v

The boundedness of the pullback of v has already been proven for $I = 0$ in Ref. [18]. The boundedness of the pullback of v for $I > 0$ can also be proven in the same way. Eq. (1a) with $C = 1 \mu\text{F}/\text{cm}^2$ can be rewritten as

$$\frac{dv}{dt} = G(t)(a(t) - v) + I + \sigma \xi(t), \quad (\text{B1})$$

where $G(t)$ and $a(t)$ are given by

$$G(t) = g_{Na} m^3 h + g_K n^4 + g_L, \quad (\text{B2})$$

$$a(t) = \frac{g_{Na} m^3 h V_{Na} + g_K n^4 V_K + g_L V_L}{G(t)}. \quad (\text{B3})$$

Here, we define v' as $v'(t) = \int_{-\infty}^t \exp(-\int_s^t G(r) dr) G(s) a(s) ds$. This is a solution of the equation:

$$\frac{dv'}{dt} = G(t)(a(t) - v'). \quad (\text{B4})$$

We also define u as

$$u(t, \omega) = \int_{-\infty}^t e^{-\gamma(t-s)} (I + \sigma \xi(s, \omega)) ds. \quad (\text{B5})$$

This is a solution of the equation:

$$\frac{du}{dt} = -\gamma u + I + \sigma \xi(t). \quad (\text{B6})$$

When we define y as $y = v - v' - u$, we have

$$\frac{dy}{dt} = -G(t)y + (\gamma - G(t))u(t, \omega). \quad (\text{B7})$$

From this equation, we have

$$\frac{dy^2}{dt} = -2G(t)y^2 + 2(\gamma - G(t))u(t, \omega)y. \quad (\text{B8})$$

Thus, we have

$$\frac{dy^2}{dt} \leq -\beta y^2 + \zeta [u(t, \omega)]^2, \quad (\text{B9})$$

where β and ζ are positive constants. From Eq. (B9) and the comparison theorem, we have

$$\phi(t, \omega) y_0 \leq e^{-\beta t} y_0^2 + \zeta \int_0^t e^{-\beta(t-s)} [u(s, \omega)]^2 ds, \quad (\text{B10})$$

where $\phi(t, \omega)$ is the map from the initial condition y_0 to $y^2(t, \omega)$. The map is defined by the solution of Eq. (B8). From Eq. (B10), we have

$$\lim_{t \rightarrow \infty} \phi(t, \theta_{-t} \omega) y_0 \leq \zeta \int_{-\infty}^0 e^{\beta s} [u(s, \omega)]^2 ds. \quad (\text{B11})$$

Eq. (B11) shows that there is a bound for the pullback of y . The pullback of v' is also bounded because $0 < g_L < G(t) < g_{Na} + g_K + g_L$ and $\min(V_{rev}) < a(t) < \max(V_{rev})$, where $V_{rev} = V_{Na}, V_K$, or V_L . From Eq. (B5), the pullback of u is given by $I/\gamma + \sigma \int_{-\infty}^0 e^{\gamma s} \xi(s) ds$. Thus, the pullback of u is bounded. Given that $v = y + v' + u$, the pullback of v is bounded.

ACKNOWLEDGMENTS

This work was supported by Tokyo Metropolitan Government Advanced Research Grant R2-2.

[1] H. Gang, T. Ditzinger, C. Z. Ning, and H. Haken, Phys. Rev. Lett. **71**, 807 (1993).
 [2] A. Longtin, Phys. Rev. E **55**, 868 (1997).
 [3] A. S. Pikovsky and J. Kurths, Phys. Rev. Lett. **78**, 775 (1997).

[4] S. G. Lee, A. Neiman, and S. Kim, Phys. Rev. E **57**, 3292 (1998).
 [5] J. L. A. Dubbeldam, B. Krauskopf, and D. Lenstra, Phys. Rev. E **60**, 6580 (1999).
 [6] J. M. Buldú, J. García-Ojalvo, C. R. Mirasso, M. C. Torrent, and J. M. Sancho, Phys. Rev. E **64**, 051109 (2001).

- [7] J. Hizanidis and E. Schöll, *Phys. Rev. E* **78**, 066205 (2008).
- [8] O. V. Ushakov, H.-J. Wünsche, F. Henneberger, I. A. Khovanov, L. Schimansky-Geier, and M. A. Zaks, *Phys. Rev. Lett.* **95**, 123903 (2005).
- [9] M. Arizaleta Arteaga, M. Valencia, M. Sciamanna, H. Thienpont, M. López-Amo, and K. Panajotov, *Phys. Rev. Lett.* **99**, 023903 (2007).
- [10] L. Kabiraj, R. Steinert, A. Saurabh, and C. Oliver Paschereit, *Phys. Rev. E* **92**, 042909 (2015).
- [11] E. Mompo, M. Ruiz-Garcia, M. Carretero, H. T. Grahn, Y. Zhang, and L. L. Bonilla, *Phys. Rev. Lett.* **121**, 086805 (2018).
- [12] Y. Zhu, V. Gupta, and L. K. B. Li, *J. Fluid Mech.* **881**, R1 (2019).
- [13] S. Luccioli, T. Kreuz, and A. Torcini, *Phys. Rev. E* **73**, 041902 (2006).
- [14] L. F. Abbott and T. B. Kepler, in *Statistical Mechanics of Neural Networks, Barcelona, 1990*, edited by L. Garrido (Springer, Berlin, 1990), pp.5-18.
- [15] L. Arnold, *Random Dynamical Systems*, (Springer-Verlag, Berlin, Heidelberg, 1998).
- [16] H. Crauel and M. Gundlach, *Stochastic Dynamics*, (Springer, New York, 1999).
- [17] T. Caraballo and X. Han, *Applied Nonautonomous and Random Dynamical Systems*, (Springer, Cham, 2017).
- [18] K. Pakdaman and S. Tanabe, *Phys. Rev. E* **64**, 050902 (2001).